Light-in-flight recording. 2: Compensation for the limited speed of the light used for observation

Nils Abramson

Equations are given for the apparent rotation and distortion of wave fronts caused by the limited speed of the light used for the observation (here referred to as a relativistic effect). Methods are discussed and mathematically derived for the compensation and the elimination of these unwanted effects. Equations are given for how these effects can be used to advantage for the manipulation of the tilt angle of the intersecting plane used in contouring. Optimization of the time resolution and the time capacity for a certain length of hologram plate is given in tabular form. A new formula is enunciated for the curvature of the relativistically distorted wave front. Finally, it is demonstrated that the ellipsoids of the holodiagram are the spherical wave fronts from a point of illumination as they are seen in a scattering medium from another point of observation.

I. Compensation of Relativistic Rotation

If an object in the shape of a flat surface travels past an observer at a velocity close to that of light (which we refer to here as relativistic velocity), it will appear both rotated and distorted. The reason is simply that the whole object is not seen simultaneously, because different points on the object surface are at different distances from the point of observation. Thus different parts of the object are seen at different points of time, and if the object's velocity is fast enough compared with that of light, it will move an observable amount during these differences in time delays.

Let us compare this effect to that of studying the stars in the sky. Neither the apparent position, nor the velocity of individual stars, nor the configuration of stars is true because we do not see them simultaneously. To observe them as they really are we would have to introduce delay lines that compensate for differences in distances.

Let us return to our initial problem which is light-in-flight recordings of fast moving objects. We shall see the closest parts of the object as if they had moved further than the more distant parts. When the velocity is that of light itself the effects are large and have to be calculated and compensated for. Thus, e.g., a flat wave front of light passing by an observer will in the first approximation appear rotated 45°. A closer study reveals that it is curved into a paraboloid with the observer at the focus. In this paper we shall study the importance of these relativistic rotations and distortions of the wave fronts and discuss methods (e.g., delay lines) to reduce, or in some cases totally eliminate, their influence on the observations.

A. Delay of Arrival Caused by the Flight Time of the Observation Beam

When the observer (B in Fig. 1) sees the wave front at W_1 it is already at W_2. When the observer looks along the line of sight he sees the light at E when it is already at D. Thus the apparent distance (R_{app}) is shorter than the real distance, if the latter is defined as the true distance at the moment of observation. Let us calculate R_{app} based on Fig. 1.

During the time it takes for the light from the wave front W_1 at E to reach the observer at B, the wave front itself has moved to position W_2. Thus: $CD = BE$.

Let BE be R_{app} (which means apparent distance R). Let BF be

$$BE = \frac{BF}{\cos(\omega - \phi)} - \frac{CD}{\cos(\omega - \phi)};$$

thus

$$R_{app} = \frac{a}{\cos(\omega - \phi)} - \frac{R_{app}}{\cos(\omega - \phi)},$$

$$R_{app} = \frac{a}{1 + \cos(\omega - \phi)}. \quad (1)$$

The author is with Royal Institute of Technology, Industrial Metrology/Production Engineering, S-100 44 Stockholm, Sweden.

Received 15 November 1983.
0003-6935/84/101481-12$02.00/0.

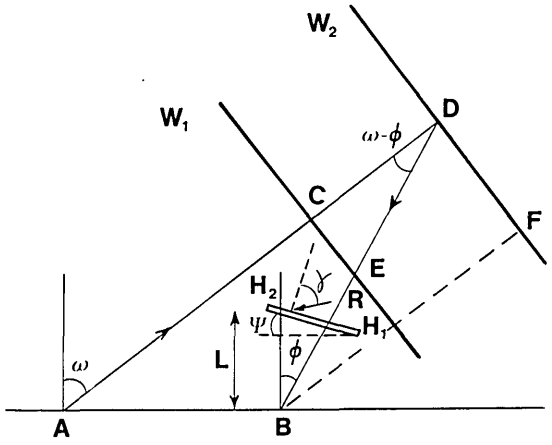

Fig. 1. Wave front (W_1) is emitted at angle ω from A and observed at angle ϕ from B. When W_1 is seen at E it is (W_2) already at D separated from B by the distance B–F which is designated a. The apparent distance in direction of observation (B–E) is designated R_{app}. Different parts on the holographic plate record the wave front at different points of time depending on the angle (γ) of the reference beam (R). Because of the distance ($L = H_2 - B$) separating the observer and the hologram plate (H_1–H_2), different viewing angles (ϕ) represent different points of time resulting from the added influence of the time of travel of the object beam and the reference beam, respectively.

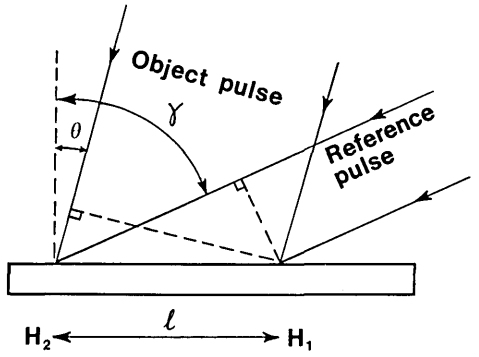

Fig. 2. Delay of recording caused by the added influence of the time of flight of the object pulse (angle θ) and the reference pulse (angle γ), respectively. The studied length (l) of the hologram plate is from H_1 to H_2.

B. Recording Delay Caused by the Flight Time of the Reference Beam

Let us study the times of arrival at a certain point on the hologram plate of the reference pulse and of the object pulse (Fig. 2).

Time for reference pulse to pass from H_1 to H_2 is t_1:

$$t_1 = \frac{1}{c}\sin\gamma;$$

Time for object pulse to pass from H_1 to H_2 is t_2:

$$t_2 = \frac{1}{c}\sin\theta.$$

Thus recorded at H_2 will be those events that happened to the object later than those recorded at H_1. The time delay (T) will be

$$T = t_1 - t_2 = \frac{1}{c}(\sin\gamma - \sin\theta) \tag{2}$$

Now let us look for maximum and minimum of T:

$$\delta T = \frac{1}{c}(\cos\gamma\delta\gamma - \cos\theta\delta\theta) = 0, \tag{3}$$

The result is the minimum for $\gamma = \theta$ which produces zero delay because the object and reference beams are parallel.

The maximum is $\gamma = -\theta$; the absolute maxima are:

$$\left.\begin{matrix}\gamma = 90, \\ \theta = -90,\end{matrix}\right\} \quad \left.\begin{matrix}\gamma = -90, \\ \theta = 90.\end{matrix}\right\}$$

These are exactly the results given by the holodiagram of Figs. 3–6. The maximum time span is reached when the plate intersects as many hyperboloids as possible, which means that the normal of the plate bisects the angle between object and reference beams. It also indicates that the k value of the holodiagram is as large as possible. In Fig. 3 this k value refers to the separation of the ellipses divided by the separation of the circles. When the separation of the ellipses is at maximum, the separation of the hyperbolas is at a minimum.

Let us now study how l of Fig. 2 depends on the observation angle ϕ if the plate has the angle ψ in relation to A B of Fig. 1:

$$l = \frac{L}{(\cos\psi)(\tan\psi + \cot\phi)}. \tag{4}$$

Thus the delay T is found by combining Eqs. (2) and (4). However, as increasing ϕ represents decreasing T the sign of T should be changed. Note that the angle (θ) between the normal of the hologram plate and the observation direction is equal to $\phi - \psi$. The angle between the normal of the hologram plate and the reference beam is still γ. Thus

$$T = \frac{L[\sin(\phi - \psi) - \sin\gamma]}{c(\cos\psi)(\tan\psi + \cot\phi)}. \tag{5}$$

C. Resulting Recorded Distance

When we make a photograph of a star that is one hundred light-years away, we record what it looked like one hundred years ago. If we want to photograph what it looks like now, this is also possible; all we have to do is to make the exposure by pressing a button that starts a clock which waits for one hundred years before taking the photograph. Recorded will be how the star looked at the moment when we pressed the button (if earth were a stable platform).

If we want to know the positions of many stars at different distances and traveling at different velocities, we could use this method of delaying the recording of each individual star in relation to its distance. With such a method we could, in theory, photograph the true positions of the stars in relation to one another at the same point of time. The practical problems would however, be immense, one being the well-known cross talk between radial and transverse velocity.

Is it possible that we could use the delay along the hologram plate in the same way as do clocks that control

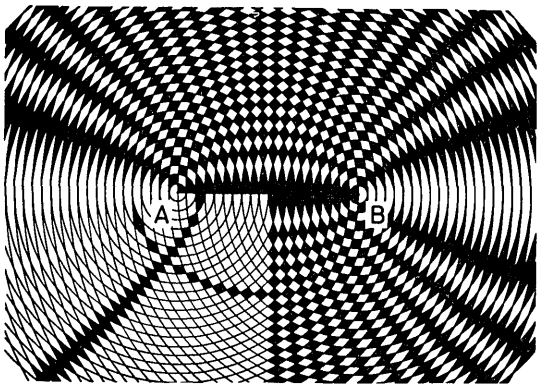

Fig. 3. A and B are the centers of two sets of concentric circles in a bipolar coordinate system. The moiré fringes form one set of hyperbolas and one set of ellipses. To emphasize these patterns, every second rhomboid area has been painted black except for one-quarter of the diagram where one ellipse and hyperbola have been marked. One rhomboid is studied in detail in Figs. 5 and 6. The circles represent spherical waves emitted from the picosecond point source A and the separation between two adjacent circles represent half of the pulse length. Then each bright ellipse represents the spherical wave (spherical pulse) as seen from B after it has been deformed by relativistic effects. This statement is true for both the curvature and the thickness (separation) of the ellipses, each one representing a consecutive point of time.

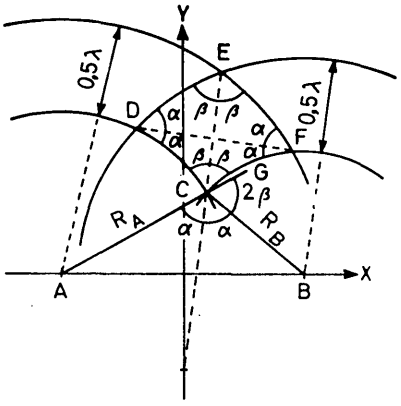

Fig. 4. Angles of one of the rhombs of Fig. 3 are studied and the two diagonals are calculated. The statements of the figure are true only if λ is infinitesimal. The distance separating the ellipses is $C - E = k \cdot R$, where R is half the pulse length. The normal to the ellipses everywhere bisect the angle ACB. The k-value is CE/0.5 λ.

the exposure of the astronomical cameras? The delay of arrival caused by the flight time of the object beam could perhaps be compensated for by the delay of the recording caused by the flight time of the reference beam. If this was possible over the whole hologram plate, we could record objects at different distances as they were at the same point of time. Let us therefore study the resulting effect when the apparent distance (R_{app}) decreases because of the flight time of the object beam [Eq. (1)] and increases because of the flight time of the reference beam [Eq. (5)]. Thus,

$$R_{app} = \frac{a}{1 + \cos(\omega - \phi)} + \frac{L[\sin(\phi - \psi) - \sin\gamma]}{\cos\psi(\tan\psi + \cot\phi)}, \qquad (6)$$

where, referring to Fig. 1,

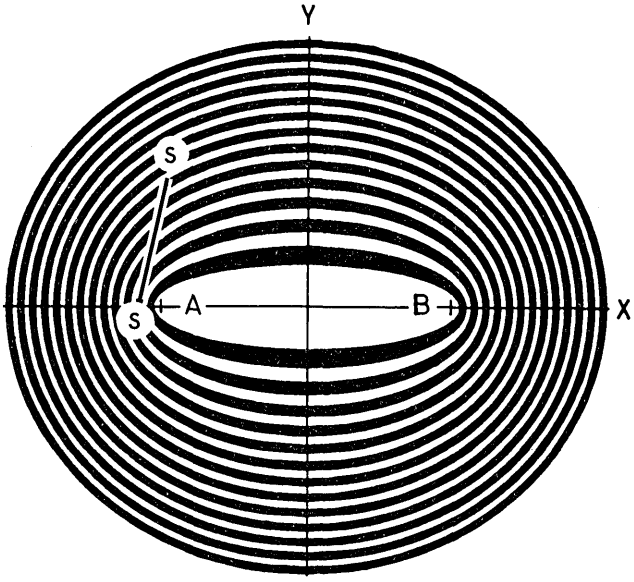

Fig. 5. Ellipsoids of the holodiagram represent the apparent wave fronts of light emitted from A and observed from B. They also represent the apparent pulse length, pulse velocity, and pulse front curvature of picosecond pulses emitted from A. When the wave front is to be studied, the object screen (S–S) should be placed with its normal toward B. Thus R_B (see Fig. 4) will be almost constant along its surface, and the intersections of the ellipsoids will be identical to those of the spheres centered at A.

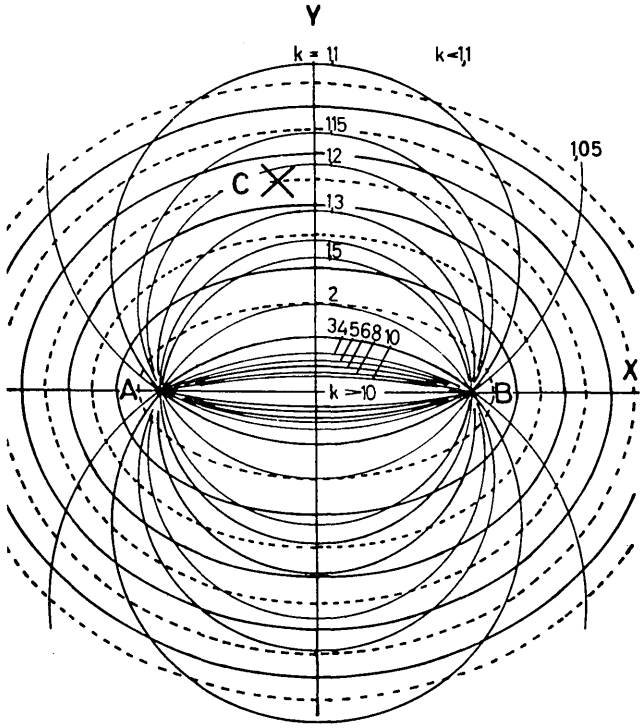

Fig. 6. Holodiagram with the arcs of circles (k circles) that represent constant separation of the ellipses. When a picosecond pulse is emitted from a point source (A) the ellipses represent the spherical pulse front as seen from B. If the true pulse length is $t \cdot c$ the apparent pulse length is $0.5\ k \cdot t \cdot c$, the apparent pulse velocity is $0.5\ k \cdot c$, and the apparent radius of curvature is $R = 2k \cdot R_A \cdot R_B/(R_A + R_B)$. The value of k is $1/\cos\alpha$ where α is found in Fig. 4.

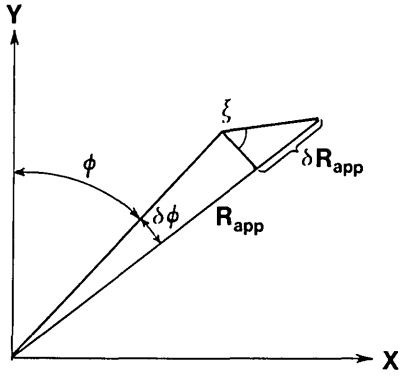

Fig. 7. See also Fig. 1. When the observation angle ϕ is increased by $\delta\phi$ the apparent distance R_{app} is increased by δR_{app}. The latter increase is caused by the combined effects of the time of flight of the observation beam (EH) and of the reference beam (R), respectively. The apparent rotation of the wave front results in the angle ξ in relation to the normal of the line of sight.

R_{app} = apparent distance from wave front to observer ($B\,E$),
a = true distance from wave front to observer ($B\,F$),
L = distance between hologram plate (H_2) and point of observation B,
ω = angle of illumination,
ϕ = angle of observation,
ψ = angle of hologram plate, and
γ = angle of reference beam.

D. Apparent Rotation of the Wave Front

Now let us look for the apparent rotation of the wave front (Fig. 7):

$$\tan\xi = \frac{\delta R_{app}}{R_{app}\delta\phi}, \tag{7}$$

ξ = apparent angle between wave front and the normal of the line of sight,
R_{app} = apparent distance, and
ϕ = angle of observation.

To find ξ let us differentiate Eq. (6):

$$\frac{\delta R_{app}}{\delta\phi} = -\frac{a\sin(\omega-\phi)}{[1+\cos(\omega-\phi)]^2} + \frac{L[\sin(\phi-\psi)-\sin\gamma][1+\cot^2\phi]}{\cos\psi(\tan\psi+\cot\phi)^2} + \frac{L\cos(\phi-\psi)}{\cos\psi(\tan\psi+\cot\phi)}. \tag{8}$$

Combining Eq. (7) with Eq. (8) and inserting the a value of Eq. (6) results in

$$\tan\xi = \frac{1}{R_{app}}\left\{\frac{-\sin(\omega-\phi)}{1+\cos(\omega-\phi)}\left[R_{app}+\frac{L[\sin\gamma-\sin(\phi-\psi)]}{\cos\psi(\tan\psi+\cot\phi)}\right] + \frac{L[\sin(\phi-\psi)-\sin\gamma][1+\cot^2\phi]}{\cos\psi(\tan\psi+\cot\phi)^2} + \frac{L\cos(\phi-\psi)}{\cos\psi(\tan\psi+\cot\phi)}\right., \tag{9}$$

where the designations are those of Eqs. (6) and (7) and Figs. 1 and 7.

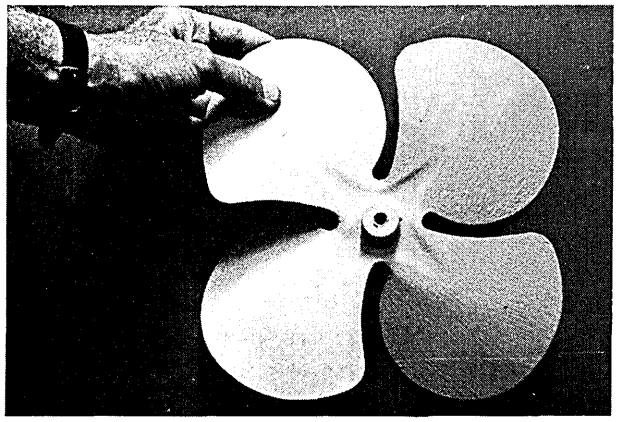

Fig. 8. Propeller of an ordinary fan used for the contouring experiment. To simplify the recording, the propeller was covered with retroreflective paint. During exposure it was rigidly fixed not handheld.

E. Examples of Compensation and Tests of Validity

1. *No Distance Between Hologram Plate and Point of Observation*

When the distance L of Fig. 1 is zero, Eq. (9) is reduced to

$$\tan\xi = -\frac{\sin(\omega-\phi)}{1+\cos(\omega-\phi)} = -\frac{2\sin\frac{\omega-\phi}{2}\cos\frac{\omega-\phi}{2}}{2\cos^2\frac{\omega-\phi}{2}} = -\tan\frac{\omega-\phi}{2}.$$

Thus

$$\xi = -\frac{\omega-\phi}{2}. \tag{10}$$

Result: There is no influence from the hologram plate. The apparent rotation is caused solely by the relativistic effect which rotates the apparent wave front from the normal to the direction of illumination until it is normal to the bisector of the illumination and observation directions. An identical result is given directly by the holodiagram (Figs. 3–6) which is simply based on ellipsoids of constant path lengths (and thus constant flight time from A to B).

2. *Light-in-Flight Recording where Illumination and Observation Directions are Perpendicular*

When our light-in-flight recordings of Figs. 1–8 in Ref. 1 were made, the flat object screen was perpendicular to the direction of observation and almost perpendicular to the wave front studied. (Object screen refers to the screen that is illuminated by the wave front to be studied.) The observation was made from such a large distance that the path length from the observer to the object screen was constant over its whole area. In this configuration, R_B of Figs. 3 and 4 is constant and R depends solely on R_A.

The relativistic 45° rotation of the wave front has no influence in that case. Thus we made no attempt to

compensate for the rotation; we just kept the camera lens as close as possible to the hologram plate so that the corresponding time of recording was as short as possible.

However, if instead we had wanted to make a 3-D study of the wave front, e.g., by recording the light it scattered when passing through a box filled with smoke, in that case the relativistic rotation of the wave front would be a great disadvantage. Is it perhaps possible to use the delay of recording along the plate to eliminate the delay of arriving of the light from the furthest parts of the smokebox? Let us study this problem mathematically.

When the angle of observation ϕ of Fig. 1 is zero, Eq. (9) is reduced to

$$\tan\xi = -\frac{\sin\omega}{1+\cos\omega} - \frac{L(\sin\gamma + \sin\psi)}{R_{app}\cos\psi}. \quad (11)$$

If the angle of illumination (ω) is perpendicular to the angle of observation (ϕ), the wave front (W_1) appears, by the relativistic effect, to be rotated 45° in the direction of ξ [Fig. 7 and Eq. (10)]. Could this rotation be compensated for by an opposite rotation caused by the hologram plate?

Inserting $\omega = 90°$ in Eq. (11) gives

$$\tan\xi = -\left[1 + \frac{L(\sin\gamma + \sin\psi)}{R_{app}\cos\psi}\right].$$

Compensation is attained when the apparent wave front is parallel to the line of observation, which is the case when the angle ξ is −90° or, in other words, when $\tan\xi = -\infty$.

Thus

$$\frac{L}{R_{app}} \cdot \frac{\sin\gamma + \sin\psi}{\cos\psi} = \infty.$$

From this equation we understand that it is impossible to reach total compensation. The closest practical approach could perhaps be for $L = 0.9R$, $\gamma = 80°$, and $\psi = 80°$. These values give

$$\tan\xi = -\left(1 + 0.9\frac{0.99 + 0.99}{0.17}\right) = -11.5,$$

$$\xi = 85°.$$

Far more practical would be to keep ψ at 45° which results in $\xi = 65°$.

Result: It is impossible to compensate totally for the relativistic rotation of 45° when illumination and observation directions are perpendicular. However, it is possible to get a partial compensation so that the rotation is decreased to 25° and in very limited cases down to 5°. Full compensation is possible for other angles of illumination and observation.

3. *Illumination and Observation Directions are Separated by 45°*

Let the illumination direction (ω) be 45° (Fig. 1). In this case is it possible to compensate so that the error in the wave front angle caused by the relativistic rotation is eliminated by the delay effect of the holographic plate? Let us study Eq. (11) again and insert $\phi = 0$; $\omega = 45°$; $\psi = 0$; $\gamma = 90$; and $\tan\xi = -1$. The result is that, for $L = 0.6R$, Eq. (11) is satisfied. Thus in this case it is possible to compensate totally for the relativistic rotation of 22.5°. However, one should keep in mind that, when a flat wave front is rotated and corrected by the hologram plate, a curved wave front will become slightly distorted by a second-order effect.

4. *Contouring, Where the Illumination and Observation Directions are Parallel*

When light-in-flight recording is used for contouring purposes it is most useful if the sheet of light that intersects the object is perpendicular to the line of sight. In that case the movable bright line of intersection is like one of the level lines of a map.

Let us return to Fig. 1 and again for simplicity set the observation angle ϕ equal to zero. Let also the illumination angle ω be zero and finally let the separation (L) between the point of observation (B) and the hologram plate (H–H) be zero. In this case Eq. (11) is reduced to

$$\tan\xi = -\frac{\sin\omega}{1+\cos\omega} = 0;$$

$$\xi = 0.$$

Thus there is no relativistic rotation when light-in-flight is used for contouring and therefore no compensation by the holographic plate is needed. However, in some cases it might be useful to be able to rotate the intersecting plane to measure and compare different angles at the object. This will be possible if we move the point of observation (B) away from the plate (H–H) so that L will no longer be zero. Let ϕ and ω still be zero. In this case Eq. (11) will be reduced to

$$\tan\xi = -\frac{L(\sin\gamma)}{R_{app}\cos\psi}.$$

If we select the following practical values: $L = 0.5R$; $\psi = 0$; and $\gamma = 90°$, the result will be $\xi = -26°$.

Thus it is practically possible to rotate the intersecting plane 25°. The absolute maximum of rotation would perhaps be when $L = R_{app}$ which simply means that the hologram plate touches the object. In this case (which is not practically useful) the angle ξ would be 45°.

Is there any possibility to get still larger rotations? Could the distance (L) from the observer to the plate be made larger than the distance (R) from the observer to the object? Yes, if we study the pseudoscopic image instead of the original virtual image. There is nothing to hinder the separation between the observer and the pseudoscopic image becoming close to zero, in which case the value of $\tan\xi$ comes close to infinity. However, other problems exist such as object image distortions that finally set a limit to the value of ξ.

Result: When light-in-flight is used for contouring, there is no problem of relativistic rotation of the intersecting plane; indeed, it is possible to utilize the effect, if desired. In that case a rotation of some 25° is practically useful in the ordinary virtual image. If larger rotation is needed the pseudoscopic image should be

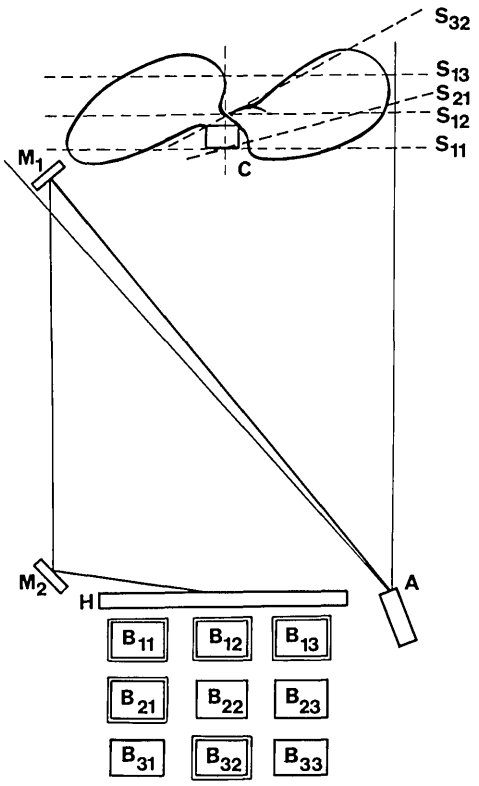

Fig. 9. Schematic view of the holographic setup. The propeller (C) of Fig. 8 is illuminated by the divergent beam from the picosecond laser (A). The reference beam is reflected by the two mirrors (M_1 and M_2) toward the hologram plate (H). In the actual experiment the distance between H and C was much longer compared with H and C than shown in this drawing. B_{ik} represent different camera positions and S_{ik} represent the corresponding intersecting surfaces.

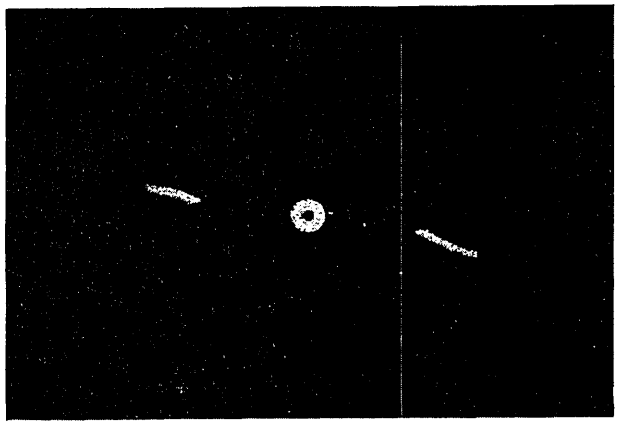

Fig. 10. When the observation is made through the hologram plate (H of Fig. 9) from a point close to its surface (B_{11}), the propeller is seen intersected by a plane (S_{11}) that is perpendicular to its axis. Illumination and observation are made from a large distance and their directions are almost parallel to the propeller shaft.

studied instead. In this case a rotation close to 45° is theoretically possible.

This ability to rotate the intersecting plane could be used to facilitate measurements, e.g., to compare the angles of an object. To demonstrate this possibility we show the propeller of Fig. 8 (from Ref. 1), the 3-D shape

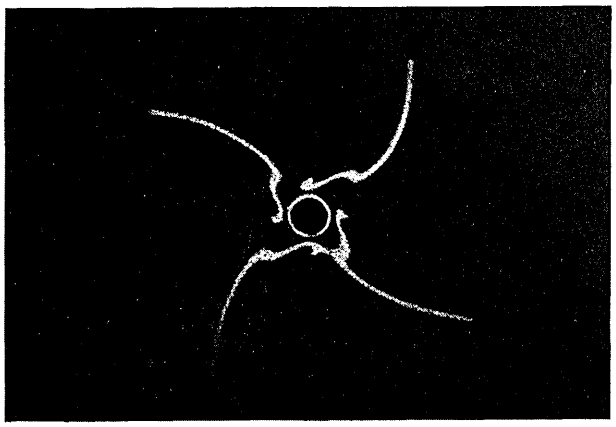

Fig. 11. Same hologram plate as in Fig. 10 but the camera is moved to position B_{12} which results in the intersecting surface being translated in depth to S_{12}.

Fig. 12. Same hologram plate as in Fig. 10 is studied from a point situated behind the plate (B_{21}) at about half of the distance the propeller was in front of the plate during the recording. In this case the intersecting surface (S_{21}) is tilted ~20°.

of which is measured from its cross sections visualized by inserting a thin sheet of light. Figure 9 is a schematic view of the holographic setup. By moving the camera along the plate the intersecting plane is translated in depth. By moving the camera away from the plate the intersecting plane is rotated.

Figure 10 shows the propeller intersected by a plane that is perpendicular to its axis. Figure 11 is photographed from the same hologram plate as Fig. 10, but the camera is translated along the plate so that the intersecting plane is moved in depth. Figure 12 shows the result when the camera, from the position of Fig. 10, is moved away from the plate instead of translated. The result is a tilt of the intersecting plane of some 20°. Figure 13 shows the result when the camera is moved still further away so that the intersecting surface is parallel to a large portion of one of the curved blades.

Finally Fig. 14 was made from the same area of the same hologram plate as Fig. 11 but during reconstruction it was photographed through two slit apertures instead of one. The resulting two parallel intersecting planes give direct information about the tilt angle. The separation of the bright lines is a function of the angle

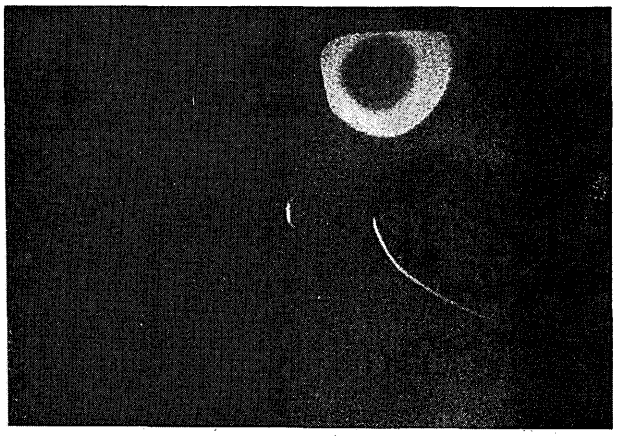

Fig. 13. Same hologram plate is in Fig. 10 but by positioning the camera still further away from the plate (B_{32}) the intersecting plane is rotated so that it becomes parallel to a large portion of one of the curved blades of the propeller.

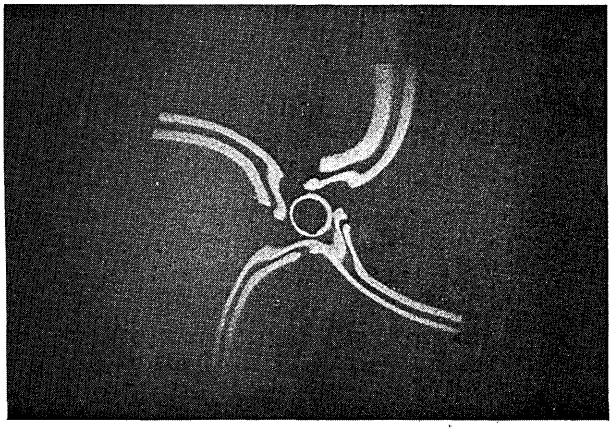

Fig. 14. Same hologram plate as in Fig. 10 was photographed with the camera in the same position (B_{12}) as in Fig. 11. However, instead of having just the ordinary single aperture, the camera was equipped with two vertical slit apertures, each 5 mm wide. The horizontal separation of the slits represents a time difference of some 20 psec and accordingly the propeller is seen intersected by two parallel surfaces separated by some 3 mm. The separation of the two lines of intersection is a measure of the angle of the object surface.

between the intersecting planes and the object surface. The larger the separation the smaller is that angle.

F. Illumination Pulse Front that is not Perpendicular to Illumination Direction

Still another possibility exists to compensate for the relativistic rotation, which is not based on the delay effect of the hologram plate and which does not distort the shape of the wave front. It can be used to compensate even when illumination and observation directions are perpendicular. This method is based on the idea of producing an illumination beam whose wave front is not perpendicular to its direction of propagation.

That statement seems absurd. We have learned from textbooks that by definition the wave fronts are always perpendicular to the rays of light and thus to the direction of travel. Thus we shall here introduce the word pulse front and use this word instead of the word wave front but only in those cases when the old definition of wave front no longer applies. Thus the bright lines of, e.g., Fig. 8 of Ref. 1 instead of referring to the wave front of light could refer to the front of a short light pulse that passed through the lens.

Very few people would dispute that the shape of the wave front or the pulse front would be the same when they pass through an ordinary lens as in the above example. The delay of the pulse front will in every point be identical to that of the wave front. However, if the lens had not been an ordinary lens with a continuous variation in thickness but instead had been a Fresnel lens or a zone lens, the wave fronts moving toward the focal point would be chopped up in small pieces of the different wave fronts that initially reached the lens. Only the continuity and the coherence of the light makes it possible for these composite wave fronts to produce a diffraction-limited point of light. If such a lens is illuminated by a short pulse of light, the pulse fronts passing through different parts of the lens will arrive at the focus at different points of time and thus no diffraction-limited point of light is produced.

Thus differences exist between wave fronts and pulse fronts. These differences only arise when the light is chopped up by discontinuities of an optical element such as Fresnel lenses, zone lenses, diffraction gratings, or holograms. The pulse front represents the shape of one single wave front, while the wave front defined as perpendicular to the level of the light represents a new composite wave front built up by the cooperative effect of many chopped up wave fronts.

Bartelt *et al.*[2] have demonstrated in an interesting experiment that the wave front of light that has been deflected by a grating is no longer perpendicular to its direction of travel. Thus the smoke-filled box inside which we want to study the 3-D shape of the wave front could be illuminated by a beam of light whose pulse front is so rotated that it compensates for the unwanted relativistic rotation.

However, we want the direction of the illumination beam, the wave front of which we want to study, to be perpendicular to the direction of the observation (same situation as in Sec. I.E.). Its wave front should be tilted so that after observation it should appear to be perpendicular to the direction of illumination.

Let us make a calculation of how such an experiment could be made. From Eq. (10) we know that the relativistic rotation in the case studied will be 45° (the angle between illumination and observation directions is bisected). Thus we shall chop up the illumination beam by a deflection in a grating so that its pulse front is rotated 45° in relation to the direction of propagation.

Let us study Fig. 15 where the illumination beam arrives at the angle $\alpha + \beta$ from the left. It illuminates the grating (g–g) and as it passes through is diffracted into a horizontal direction. The wave front (W_1) enters the grating at angle α and leaves it at angle β. The pulse front is rotated at an angle γ.

The path length of the lowest ray is the distance $a + b$ longer than the highest ray. Thus, after diffraction the lowest part of the beam will be delayed the distance

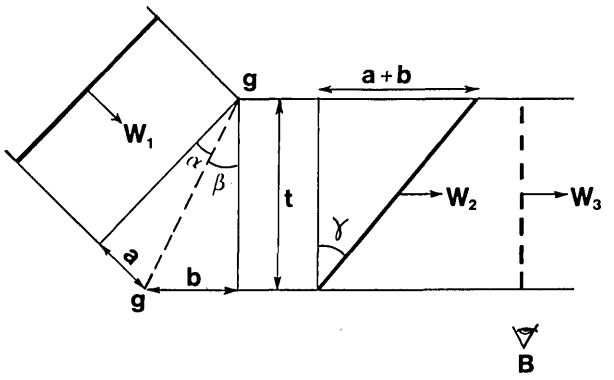

Fig. 15. Studied beam arrives at the angle α to the normal of the grating g–g with the length l. It leaves the grating at the angle β resulting in a total deflection of $\alpha + \beta$. The original wave front (W_1) is transformed into the new (wave front) pulse front (W_2) which is tilted at an angle γ relative to the direction of propagation. When this tilted (wave front) pulse front is observed from B it appears normal to the propagation (W_3) because of the relativistic effect.

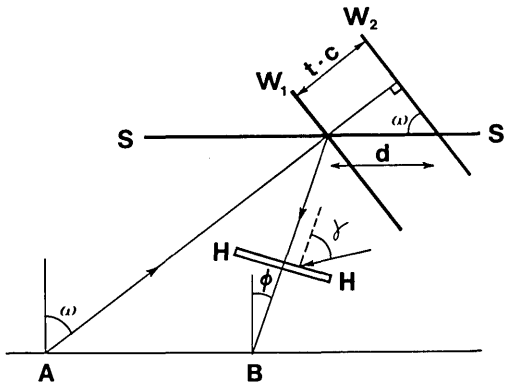

Fig. 16. Apparent pulse width (d) seen on the screen (S–S) generally depends on the angle of illumination (ω), the angle of observatioin (ϕ), and the angle (γ) of the reference beam (R). It also depends on the distance between the hologram plate H–H and the point of observation (B). We study only the special case when this distance is zero and ϕ also is zero.

$a + b$, resulting in the tilt angle γ of the pulse front. Let the illuminated length of the grating be l and the thickness of the diffracted beam be t. Thus

$$\left.\begin{aligned} a &= l\sin\alpha, \\ b &= l\sin\beta, \\ t &= l\cos\beta, \\ \tan\gamma &= \frac{a+b}{t}, \\ \tan\gamma &= \frac{\sin\alpha + \sin\beta}{\cos\beta}. \end{aligned}\right\} \tag{11}$$

For simplicity set $\alpha = \beta$ which results in $\gamma = 2\alpha$.

Thus the rotation of the pulse front is equal to the deflection of the beam or, in other words, the pulse front is kept parallel to itself independent of the changes in propagation directions caused by diffraction. These statements, however, are true only when $\alpha = \beta$ or $\alpha = 0$.

Results: The illumination beam should be deflected at 45° by a grating bisecting this angle. The result will be a beam whose pulse front is rotated 45°. The relativistic rotation of the pulse front will be of the same value but opposite direction, which results in the wave front appearing to an observer at B at its true angle.

II. Time Resolution

Let us study Fig. 16 which differs from Fig. 1 in that W_1 and W_2 now represent the simultaneous front and back of a light pulse. This pulse is emitted from A at the angle ω and its projection on the screen (S–S) is observed from B at the angle ϕ.

This time we shall not try to find the general solution to the observed pulse width (d) but only study the special case when ϕ is close to zero. Thus the object screen S–S is perpendicular to the direction of observation and therefore the relativistic rotation has no influence on d (see also Fig. 3). Further on, the point of observation is so close to the hologram plate (H–H)

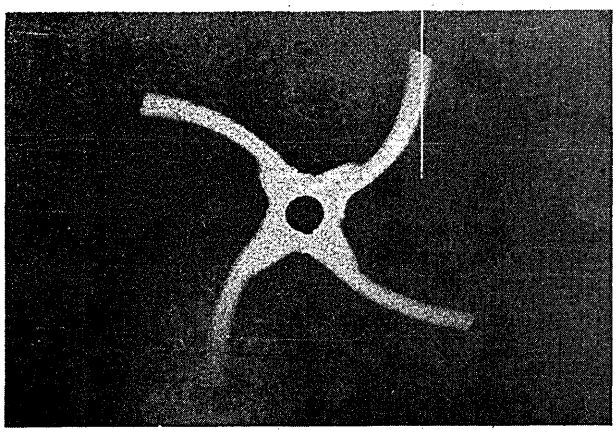

Fig. 17. Shorter pulse produces a thinner line of intersection on the surface of the object. To resolve a thin line a large aperture is needed, which uses a larger area on the hologram plate. The resulting photographic image corresponds to a longer recording time, which again results in a broader line. One therefore has to compromise and seek for the optimum aperture. The photograph is made from the same reconstruction as that of Fig. 11, but too large an aperture has broadened the line of intersection.

that the delay of the reference beam (R) along the plate will produce no rotation either.

The true length of the pulse is $t \cdot c$, its projection on the screen is

$$d = \frac{tc}{\sin\omega}, \tag{12}$$

where d = projection of pulse on the object screen,
t = time duration of pulse,
c = speed of light, and
ω = illumination direction.

When we are looking through a hologram plate, different parts of the observing aperture see what was recorded at different points of time. If a slit aperture is used, the broader the slit and the larger the angle of the reference pulse the longer will be the corresponding observation time. As an example study Fig. 17 which is photographed from the same area of the same holo-

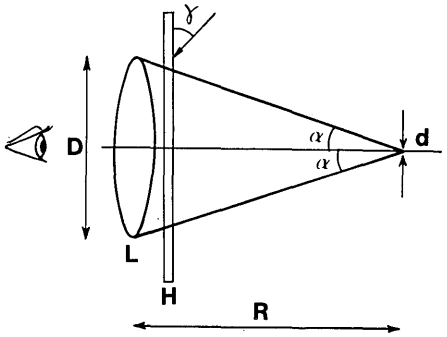

Fig. 18. Resolution (d) of a lens (L) with the diameter D positioned close to the hologram plate (H) is calculated from the observation angle (2α) and the distance (R). At the hologram plate, (D) represents a time difference depending on the angle (γ) of the reference beam. Line broadening is caused both by limited aperture resolution and by time smear. The resolving power is optimized when the conditions are such that these two effects are equal.

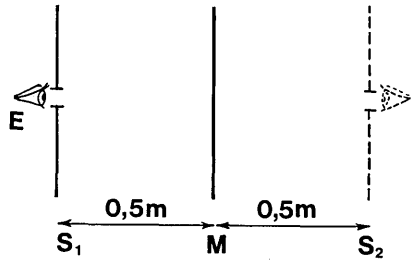

Fig. 19. Looking through a slit at a slit; an eye (E) looks through a slit (S_1) with width (d) at the mirror image of this slit (S_2). The mirror M is placed so that the distance separating the observing slit (S_1) and the observed slit (S_2) is 1 m. What is the minimum slit that can be resolved through the limited width of the slit itself? This problem is identical to: What is the shortest light pulse that can be resolved if the illumination of the object screen and the hologram plate are identical?

gram as Fig. 11. The use of a larger aperture, however, results in a decrease of resolution.

On the other hand, the shorter the illumination pulse the thinner will be the bright line representing the wave front and the larger is the observation aperture needed to resolve that line during reconstruction. These two effects set opposite demands on the slit width. To see a thin line we need a large aperture which causes a broadening of the line. Thus we have to reach a compromise. Let us accept that the studied linewidth appears broadened to twice its true thickness because the width of the aperture slit represents a certain duration of recording time.

A. Aperture Width

An ordinary circular aperture has by definition the following resolution:

$$d = \frac{1.22\lambda}{2\sin\alpha}, \tag{13}$$

where d = diffraction-limited resolution,
λ = wavelength of light, and
α = half of the observation angle as defined in Fig. 18.

A slit aperture is used and the factor 1.22, which refers to a circular one, is excluded for the sake of simplification. We also make the approximation $2\sin\alpha \sim D/R$. Then the combination of Eqs. (12) and (13) results in

$$D = \frac{\lambda R \sin\omega}{t \cdot c}. \tag{14}$$

Thus D is the length of the hologram plate (aperture slit width) needed to resolve the pulse of the duration t.

Now let us study how long recording time (T) is represented by D. This has already been calculated in Eq. (2):

$$T = \frac{L}{C}[\sin\gamma - \sin\theta],$$

where T is the recording time over the distance l along the plate (see Fig. 2). Insert $l = D$ and $\theta = \phi - \psi$, so

$$T = \frac{1}{c}[\sin\gamma - \sin(\phi - \psi)]. \tag{15}$$

Now finally let us combine Eqs. (14) and (15) while inserting $T = t$, corresponding to equal apparent pulse width caused by the true pulse length and by the recording time caused by the observation aperture slit width:

$$\sin\gamma = \frac{t^2c^2}{\lambda R \sin\omega} + \sin(\phi - \psi), \tag{16}$$

where γ = reference beam angle (Figs. 5 and 6),
t = pulse duration,
R = distance separating object screen from observation,
ω = illumination direction,
ϕ = observation direction, and
ψ = hologram angle.

In this equation γ represents the largest angle (Fig. 16) allowed for the reference beam in order that the apparent linewidth should not become more than twice the true linewidth.

B. Examples of Linewidths and Tests of Validity

Equation (13) has been used to calculate the minimum observation slit aperture needed during reconstruction to resolve the linewidth caused by a certain pulse direction (t). Let us use this equation to find out what is the minimum slit width through which we can resolve another slit of the same width 1 m away (Fig. 19). In other words, if we stand in front of a mirror that is 0.5 m away and look through a slit at the mirror image of that slit, what would be the narrowest slit that could be resolved? Again, start with Eq. (13) and exclude the constant 1.22 which refers to a circular aperture. Insert $2\sin\alpha = D/R$ (Fig. 18), and $d = D$ which means that the studied slit has the same width as the slit through which the observation is made. Finally insert the distance R = 1 m:

$$d^2 = \lambda \cdot R,$$

$$d = \sqrt{0.6328}\,10^{-6},$$

$$d = 0.8 \text{ mm}.$$

Table I. Distance to Object Screen (R) is 1 m

t (sec)	$t \cdot c$ (m)	D (m)	sineγ	T	n
2×10^{-15}	6×10^{-7}	$1.2 \times$	57×10^{-8}	19×10^{-16}	0.81
10^{-14}	3×10^{-6}	2.1×10^{-1}	14×10^{-6}	48×10^{-15}	4.8
10^{-13}	3×10^{-5}	2.1×10^{-2}	14×10^{-4}	48×10^{-13}	48
10^{-12}	3×10^{-4}	2.1×10^{-3}	14×10^{-2}	48×10^{-11}	480
2.7×10^{-12}	8.1×10^{-4}	8.1×10^{-4}	1	33×10^{-10}	1250
10^{-11}	3×10^{-3}	2.1×10^{-4}	1	33×10^{-10}	333
10^{-10}	3×10^{-2}	2.1×10^{-5}	1	33×10^{-10}	33
10^{-9}	3×10^{-1}	2.1×10^{-6}	1	33×10^{-10}	3.3

t = pulse duration,
$t \cdot c$ = pulse length,
D = aperture width,
sineγ = sine of reference beam direction,
T = time capacitance of 1-m hologram plate,
n = number of information frames per meter of hologram plate.

Thus the 0.8-mm wide aperture slit has the unique property of producing minimum apparent slit width when viewed through itself from a distance of 1 m. Had the viewing distance instead been only 10 mm the corresponding slit width would be 0.08 mm.

Let us finally study the time capacity of the hologram plate when different pulse lengths are to be resolved.

When the studied pulse is very short a large observation aperture slit is needed and therefore the number of information frames is low (if we define an information frame as the length along the hologram plate needed to resolve the linewidth of the pulse).

When the studied pulse is very long only a small aperture slit is needed. On the other hand the studied linewidth will be broad and the number of information frames will for this reason be low. (This time if we define an information frame as the length along the hologram plate we have to move the aperture slit in order to move the pulse one pulse width.)

In between these two extremes there are pulse widths corresponding to large numbers of information frames. The maximum appears at the two previously calculated values of 0.8 mm at 1-m distance and 0.08 mm at 1-cm distance. The results of our calculations are given in Table I. The shorter the distance (R) between hologram plate and object screen the higher is the resolution. If this distance is zero the resolution can be of the order of one wavelength. Such a configuration is described in Ref. 3, where the hologram plate itself is used as object screen. In such a case, however, the number of information frames will be unity.

III. Relativistic Distortion of Wave Fronts

A flat surface traveling at relativistic velocity past an observer will not only appear rotated but also distorted into a complex curvature. The reason for this effect is the motion of the object during the time delays caused by different path lengths for the light traveling from the surface to the point of observation. These time delays result in the apparent distances to points on the surface differing from the true distances as described in Eq. (1), where the studied surface is the wave front of light. The apparent distance is a result of the true distance, the angle of illumination, and the angle of observation. Thus also the apparent curvature is a function of these parameters.

The curvature of the aparent (relativistically distorted) wave front can be calculated mathematically, e.g., by integrating the rotations of infinitesimal areas using, e.g., Eq. (9), but this is an indirect and complex method. For this reason most of the calculations made in this paper have been limited to a constant illumination direction (ω = constant) and one simple direction of observation ($\phi = 0$).

However, a simple device already exists for calculating the angle and the 3-D curvature of the apparent wave fronts and this device is the holodiagram.[4]

A. Holodiagram

The holodiagram (Figs. 5 and 6) is based on ellipsoids representing the locus of constant path length for light traveling from the point source of illumination A to the point of observation B. Thus all the light from A reflected by one of these ellipsoids will arrive at B after the same traveling time. This statement is true independent of whether the reflection is specular or diffuse. If an ultrashort spherical light pulse is emitted from A, one single totally illuminated ellipsoidal surface at a time would be seen from B.

Thus the ellipsoids of the holodiagram represent the relativistically distorted spherical wave fronts emitted from A and observed from B.

To minimize the distortion of a wave front the object screen should be placed so that all points on its flat surface are the same distance from B. This is the case when the object screen is at a large distance from B and at such an angle that its normal is directed toward B. Such was the configuration when Figs. 3 and 8 of Ref. 1 were made. The object screen was close to A but distant from B; its normal was directed toward B. The result was that the wave fronts from A appeared undistorted. Spherical waves from A were represented by circular intersections of the rotational symmetric ellipsoids. From the construction of the ellipsoids of Figs. 3 and 4 it is easy to understand that, when R_B is constant, the intersections of the ellipsoids are identical to those of the spherical waves emitted from A.

The properties of the holodiagram have been described before (see, e.g., Ref. 4, Secs. 4 and 5). Points

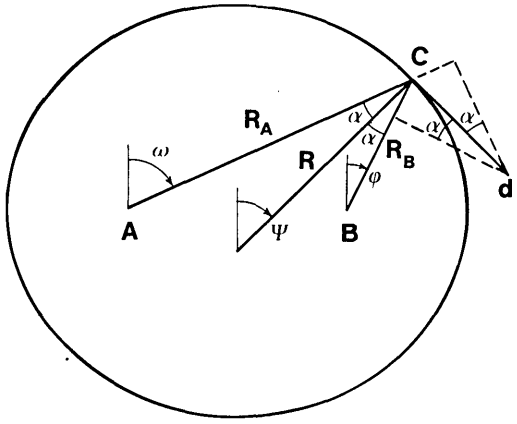

Fig. 20. Radius of curvature (R) of the ellipsoids of the holodiagram at any general point (C) is calculated from the distance (R_A) to the point of illumination (A), the distance (R_B) to the point of observation (B), and the knowledge that R bisects ACB. The radius R represents the apparent direction of light and the apparent curvature of wave fronts that in reality come from A and have a radius of curvature that is R_A.

A and B of Fig. 6 are the focal points of a set of rotational symmetric ellipsoids each representing a path length that is one wavelength longer than that of the adjacent smaller ellipsoid. The separation of the ellipsoids is $k \cdot 0.5\lambda$, where the numerical value of k is constant along arcs of circles and printed in the diagram. The value of k is

$$k = 1/\cos\alpha, \tag{17}$$

where 2α is the angle (ACB of Fig. 4) separating the direction of illumination and the direction of observation. The direction of maximal interferometric sensitivity to displacements is along the normal to the ellipsoids which is identical with the bisector of ACB. The displacement of an object point that has been twice exposed in a hologram is calculated as follows:

$$d = n \cdot k \cdot \frac{\lambda}{2}, \tag{18}$$

where n = number of interference fringes between fixed and displaced points on the object,
λ = wavelength of light, and
k = k value from the holodiagram.

When the object is large the curvature of the ellipsoids results in different parts having different k values and different angles of sensitivity. Thus it is important to know the curvature of the ellipsoids not only for light-in-flight recordings but also for hologram interferometry.

Knowing that the ellipsoids are the wave fronts from (A) as observed from (B) it is not surprising that hologram interference fringes as seen from (B) are a result of changes in the intersections of the object made by the ellipsoids. When the point of observation is changed the focal point (B) of the ellipsoids changes. Consequently the hologram interference pattern seen on the object depends on the point of observation.

B. Radius of Curvature

Let us study Fig. 20 and calculate the radius of curvature (R) of one ellipse as a function of the distance and direction of illumination (R_A) and the distance and direction of observation (R_B).

We start with the knowledge, perhaps easiest found in the holodiagram, that R bisects the angle ACB. [The diagonals of a rhomb (Fig. 4) bisect the angle between two adjacent sides.] Another condition is that all three radii should intersect at C; if therefore C is moved a small distance (d) along the tangent of the ellipse all the radii rotate at such angles that their motion at C is equal to the projection of d on their normals:

$$2\delta\psi = \delta\omega + \delta\phi,$$

$$\delta\psi = d/R,$$

$$\delta\omega = \frac{d\cos\alpha}{R_A},$$

$$\delta\phi = \frac{d\cos\alpha}{R_B},$$

$$k = \frac{1}{\cos\alpha}.$$

Thus

$$\frac{2k}{R} = \frac{1}{R_A} + \frac{1}{R_B}, \tag{19}$$

or

$$R = 2k\frac{R_A \cdot R_B}{R_A + R_B}, \tag{20}$$

where R = radius of curvature of ellipse,
R_A = radius of wave front of illumination beam,
R_B = radius of wave front of observation beam, and
k = the usual constant of the k circles of the holodiagram.

Let us set this new rule of the holodiagram in words: The curvature of the ellipse at C multiplied by $2k$ is equal to the sum of the curvature of the illumination beam and the curvature of the observation beam.

This statement is true not only for the ellipse but for any optical case as we will see in the following.

1. *Separation of* A *and* B *is Small*

Let us now study the conventional equation of an ellipse:

$$\frac{x^2}{a^2} + \frac{y^2}{b^2} = 1, \tag{21}$$

where a and b are the intersections of the ellipse by the x axis and y axis, respectively.

When the separation of A and B is zero, the factors a and b are equal ($b = a$) and thus the ellipse is transformed into a circle ($R = a$). We get the same result from Eq. (20) with inserted $R_A = R_B$ and $k = 1$. Thus, if the point of illumination and the point of observation are very close together, the apparent wave front will be identical to the true wave front and the relativistic distortion is zero. This configuration is therefore ad-

vantageous and it was used for the contouring method described in Sec. I.E.4.

To make the intersecting surfaces as flat as possible the distances to the point of illumination and that of observation should be large. If R_A and R_B of Eq. (20) are infinite, R also is infinite and the curvature is zero. Thus, for contouring purposes, the intersecting surfaces can be made flat by using collimated illumination and observation.

From Eq. (20) it is, however, evident that another condition exists that also produces intersecting surfaces that are flat, namely, when R_A and R_B are equal but of different sign. Such is the case if, e.g., the illumination beam is converging toward a point that is situated at the same distance behind the object surface as the observation point is situated in front of it.

Thus, we have shown two ways to produce intersecting surfaces that appear flat to the observer. Either illumination and observation should be collimated or they should be spherical with the same radius but different sign. When used for large objects these two methods, however, have the disadvantage that they need collimating or focusing optics of a size that is at least as large as the area of the object studied. However, a third method that does not have this drawback exists based on manipulation of the reference beam.

Light-in-flight recordings differ from ordinary holograms in that they are influenced by the angle and direction of the reference beam. (This is not the case for ordinary holograms; they are indifferent to the properties of the reference beam as long as it is identical to the reconstruction beam.) Thus a properly shaped reference beam can be used to correct for the out-of-flatness of the apparent intersecting light surface without distorting the image of the object. The calculation of the needed shape and curvature of such a reference beam is quite complicated and outside the scope of this paper.

However, when the contouring method is combined with observation by a TV camera interconnected to a computer, the intersection by an apparent spherical light sheet might be just as useful as by a flat one. The transformation from spherical to orthogonal coordinates should produce no problems.

2. *Separation of* A *and* B *is Large*

When the separation of A and B is infinite the factor a of Eq. (21) becomes infinie and the ellipse in the vicinity of B is transformed into a parabola. Thus, if the point of illumination (A) is distant (collimated illumination) the plane waves from A are, by relativistic effect, transformed into paraboloids with B at its focus. The radius of curvature of this paraboloid is $k \cdot R_B$, where R_B is the distance to the point of observation (B). To make the apparent wave front (with the radius R) as identical as possible to the true wave front (with an infinite radius) the distance from object screen to the observer (R_B) should also be large.

IV. Summary

An equation is given for the relativistic rotation as a result of the delay of arrival caused by the flight time of the object beam. Another equation is given for the delay of recording caused by the flight time of the reference beam. It is demonstrated how the combination of these two equations produces the resulting apparent wave front.

Calculations are used to find different holographic configurations for which the relativistic rotation can be compensated for and in some cases totally eliminated. It is also mathematically demonstrated how the rotation can be used to an advantage, e.g., to manipulate the tilt angle of the intersecting plane when light-in-flight is used for contouring purposes.

The time resolution of light-in-flight recording by holography is studied mathematically, and it is demonstrated that the resolution is a function of the aperture of the camera used in the reconstruction stage. The larger the aperture, the higher is the optical resolution of the thin line representing the wave front. On the other hand, a large aperture covers a large part of the hologram plate and thus represents a longer observation time which again lowers the time resolution. For every pulse width there exists a certain optimal angle of the reference beam and an optimal aperture width. These factors are given in a table that also describes how a certain length of hologram plate can be utilized either to produce a high time resolution or a high time capacity.

The relativistic distortion of wave fronts is also studied and it is demonstrated that the spherical wave front is distorted into one of the ellipsoids of the holodiagram. A new equation for the curvature of these ellipsoids is presented. Direct knowledge of the holodiagram can be utilized not only for hologram interferometry but also for the study of the relativistic distortion of wave fronts.

Finally, it should be pointed out that the calculations and the descriptions of curvatures of pulse fronts are identical for light of short duration, for light of short coherence length, and for the intersecting surfaces used in two-frequency contouring.

The experiments described in this paper were all carried out by the author at the Royal Institute of Technology, Stockholm and at the Spectra-Physics Laboratory, Mountain View, California. The work was sponsored by the Swedish Board for Technical Development whose interest and support is gratefully acknowledged.

References

1. N. Abramson, Appl. Opt. **22,** 215 (1983).
2. H. A. Bartelt, S. K. Case, and A. W. Lohmann, Opt. Commun. **30,** 13 (1979).
3. R. Salazar and G. Tribillon, Opt. Commun. **45,** 26 (1983).
4. N. Abramson, *The Making and Evaluation of Holograms* (Academic, London, 1981).